

1-1-2000

Structural Characterization of Rapid Thermal Oxidized $\text{Si}_{1-x-y}\text{Ge}_x\text{C}_y$ Alloy Films Grown by Rapid Thermal Chemical Vapor Deposition

W. K. Choi

J. H. Chen

L. K. Bera

W. Feng

K. L. Pey

See next page for additional authors

Follow this and additional works at: <https://scholarcommons.scu.edu/elec>

Recommended Citation

W.K. Choi, J.H. Chen, L.K. Bera, W. Feng, K.L. Pey, J. Mi, C.Y. Yang, A. Ramam, S.J. Chua, J.S. Pan, A.T.S. Wee, and R. Liu, "Structural Characterization of Rapid Thermal Oxidized $\text{Si}_{1-x-y}\text{Ge}_x\text{C}_y$ Alloy Films grown by Rapid Thermal Chemical Vapor Deposition," Journal of Applied Physics 87, 192-197 (2000).

Copyright © 2000 American Institute of Physics Publishing. Reprinted with permission.

This Article is brought to you for free and open access by the School of Engineering at Scholar Commons. It has been accepted for inclusion in Electrical Engineering by an authorized administrator of Scholar Commons. For more information, please contact rscroggin@scu.edu.

Authors

W. K. Choi, J. H. Chen, L. K. Bera, W. Feng, K. L. Pey, J. Mi, Cary Y. Yang, A. Ramam, S. J. Chua, J. S. Pan, A. T.S. Wee, and R Liu

Structural characterization of rapid thermal oxidized $\text{Si}_{1-x-y}\text{Ge}_x\text{C}_y$ alloy films grown by rapid thermal chemical vapor deposition

W. K. Choi, J. H. Chen, L. K. Bera, W. Feng, and K. L. Pey

Microelectronics Laboratory, Department of Electrical Engineering, National University of Singapore, 4 Engineering Drive 3, Singapore 117576

J. Mi and C. Y. Yang

Microelectronics Laboratory, Santa Clara University, 500 El Camino Real, Santa Clara, California 95053

A. Ramam, S. J. Chua, and J. S. Pan

IMRE, Blk S7, Level 3, NUS, Singapore 119260

A. T. S. Wee and R. Liu

Surface Science Laboratory, Department of Physics, National University of Singapore, 10 Kent Ridge Crescent, Singapore 119260

(Received 14 June 1999; accepted for publication 27 September 1999)

The structural properties of as-grown and rapid thermal oxidized $\text{Si}_{1-x-y}\text{Ge}_x\text{C}_y$ epitaxial layers have been examined using a combination of infrared, x-ray photoelectron, x-ray diffraction, secondary ion mass spectroscopy, and Raman spectroscopy techniques. Carbon incorporation into the $\text{Si}_{1-x-y}\text{Ge}_x\text{C}_y$ system can lead to compressive or tensile strain in the film. The structural properties of the oxidized $\text{Si}_{1-x-y}\text{Ge}_x\text{C}_y$ film depend on the type of strain (i.e., carbon concentration) of the as-prepared film. For compressive or fully compensated films, the oxidation process drastically reduces the carbon content so that the oxidized films closely resemble to $\text{Si}_{1-x}\text{Ge}_x$ films. For tensile films, two broad regions, one with carbon content higher and the other lower than that required for full strain compensation, coexist in the oxidized films. © 2000 American Institute of Physics. [S0021-8979(00)08201-3]

I. INTRODUCTION

It has been demonstrated that epitaxial $\text{Si}_{1-x}\text{Ge}_x/\text{Si}$ heterostructures have provided impressive results for Si-based band-gap engineering.¹ The heterostructures have created a great deal of interest as it can be readily incorporated into standard integrated circuit fabrication processes. For instance, high speed (75 GHz) electronic circuits have been fabricated with heterostructure $\text{Si}_{1-x}\text{Ge}_x/\text{Si}$ bipolar transistors.² Other devices fabricated using $\text{Si}_{1-x}\text{Ge}_x/\text{Si}$ heterojunction technology include infrared detectors^{3,4} and high electron mobility structures.⁵

The electronic properties of the heterostructure devices are very sensitive to the band alignment at the heterointerface and the band gap of $\text{Si}_{1-x}\text{Ge}_x$ which in turn depends on the elastic strain in the epilayers. The strain is metastable and high-temperature processing steps can cause the strain relaxation. This will create misfit dislocations and can degrade the electronic properties of the heterostructure devices.^{6,7}

The incorporation of carbon (C) in $\text{Si}_{1-x}\text{Ge}_x$ layers allows the growth of heterostructures with well-controlled misfit strain. $\text{Si}_{1-x-y}\text{Ge}_x\text{C}_y$ epilayers have been formed by molecular-beam epitaxy^{8,9} and rapid thermal chemical vapor deposition (RTCVD)¹⁰ techniques. The growth of C-containing epitaxial alloy layers is, however, difficult due to the high mismatch between the C and Si lattices, low solubility of C in Si, and the tendency of silicon carbide (SiC) precipitation.

Rapid thermal processing as a low thermal budget technique is widely used in the manufacturing of advanced semi-

conductor devices.¹¹ For a thin $\text{Si}_{1-x}\text{Ge}_x$ strained layer, a short high-temperature process may be desirable as it creates less misfit dislocations.^{6,12} For this reason, there are reports on rapid thermal oxidation^{13,14} or annealing¹⁵ of strained $\text{Si}_{1-x}\text{Ge}_x$ layers. So far, no report is available in the rapid thermal oxidation of epitaxial $\text{Si}_{1-x-y}\text{Ge}_x\text{C}_y$ films. In this work, we present the structural results of as-prepared and rapid thermal oxidized $\text{Si}_{1-x-y}\text{Ge}_x\text{C}_y$ alloy films grown by RTCVD technique.

II. EXPERIMENT

The $\text{Si}_{1-x-y}\text{Ge}_x\text{C}_y$ samples were epitaxially grown on *n*-type (100) Si substrates by RTCVD. Details of the growth procedure can be found elsewhere.¹⁰ Before epitaxy growth, an *in situ* hydrogen bake at 1050 °C for 30 s was performed to remove the native oxide and other impurities from the Si surface. During growth, the substrate was heated with a bank of halogen lamps and the growth temperature and pressure of the alloy layers were 550–600 °C and 1.5 Torr, respectively. The process gases were silane (SiH_4), germane (GeH_4), methylsilane (SiCH_3), and hydrogen (H_2). A Si buffer layer (200 nm) was grown at 900 °C, followed by the growth of the alloy layer. In this work, we report mostly the structural results of $\text{Si}_{0.887-y}\text{Ge}_{0.113}\text{C}_y$ (i.e., 11.3 at.% of Ge and $0 \leq y \leq 0.0184$) samples. The results of two 20 at.% Ge samples ($\text{Si}_{0.8}\text{Ge}_{0.2}$ and $\text{Si}_{0.784}\text{Ge}_{0.2}\text{C}_{0.016}$) have also been included for comparison. The alloy thickness was in the range of 95–130 nm.

Rapid thermal oxidation (RTO) was carried out in dry oxygen ambient with an AST SHS 10 rapid thermal processor. The system consists of double-sided tungsten halogen lamp heater with independent top and bottom lamp bank control. A quartz reactor chamber is installed in a highly reflecting, gold-plated reactor block. The $\text{Si}_{1-x-y}\text{Ge}_x\text{C}_y$ samples were placed on top of a 4 in. wafer. The oxidation temperature control was obtained with the help of a pyrometer. RTO was performed at 1000 °C for 270 s in dry oxygen ambient. The oxide thickness was found to be between 10 and 16 nm.

The infrared (IR) measurements were carried out using a Fourier transform infrared spectrometer (Nicolet Magna IR750). The x-ray photoelectron spectroscopy (XPS) measurements were performed using a VG ESCALAB MKII spectrometer. A Mg $K\alpha$ source was used with the analyzer mode set at a constant analyzer energy of 20 eV. The x-ray source was run at 120 W and a takeoff angle of 75°. All the XPS spectra were fitted with Gaussian functions and the background was removed by the Shirley subtraction method.

The x-ray diffraction (XRD) measurements were carried out on a Philips high-resolution x-ray diffraction system. The system is equipped with optical coding and Bartel's crystal [Ge(220)] which ensures fine precision (0.0001°) and high monochromatic beam (peak broadening of 12 arcsec) for the rocking curve scans. The Ω -2 θ scans were performed around the symmetrical planes of (004) with the silicon substrate giving a peak at a Bragg angle of 34.5959°. The Raman measurement was performed at room temperature in the backscattering configuration at the (100) face using a 488 nm line from an Ar⁺ laser. The spectra were recorded using a SPEX Raman spectrometer equipped with a double monochromator and observed with a multichannel detector.

III. RESULTS AND DISCUSSION

A. As-prepared samples

Figure 1(a) shows the IR absorption spectra of all the as-prepared $\text{Si}_{0.887-y}\text{Ge}_{0.113}\text{C}_y$ samples. The carbon absorption peak at 607 cm^{-1} was absent for sample $\text{Si}_{0.887}\text{Ge}_{0.113}$ as no carbon was introduced into the film during growth. The spectra of $\text{Si}_{0.8811}\text{Ge}_{0.113}\text{C}_{0.0059}$ and $\text{Si}_{0.8738}\text{Ge}_{0.113}\text{C}_{0.0132}$ show sharp carbon peak. This means that carbon is incorporated substitutionally into the films. The carbon peak of $\text{Si}_{0.8811}\text{Ge}_{0.113}\text{C}_{0.0184}$ is shifted to 616 cm^{-1} and is broader than that of samples $\text{Si}_{0.8811}\text{Ge}_{0.113}\text{C}_{0.0059}$ and $\text{Si}_{0.8738}\text{Ge}_{0.113}\text{C}_{0.0132}$. We believe the shift and the broadening of the peak is closely related to the carbon concentration in the film. This will be discussed in the next paragraph. It is important to note that we observed no SiC precipitate formation in all the as-prepared samples as the SiC stretching mode is absent in all the spectra in Fig. 1(a). The XPS analysis on the as-prepared samples gave the silicon, germanium concentrations agreed with that obtained from secondary ion mass spectroscopy (SIMS) experiments.¹⁰ The XPS measurements, however, cannot provide accurate estimation for the rather low carbon concentration in the films.

Figure 2 shows the (004) reflection x-ray rocking curves of the $\text{Si}_{0.887-y}\text{Ge}_{0.113}\text{C}_y$ alloy films. The peak of

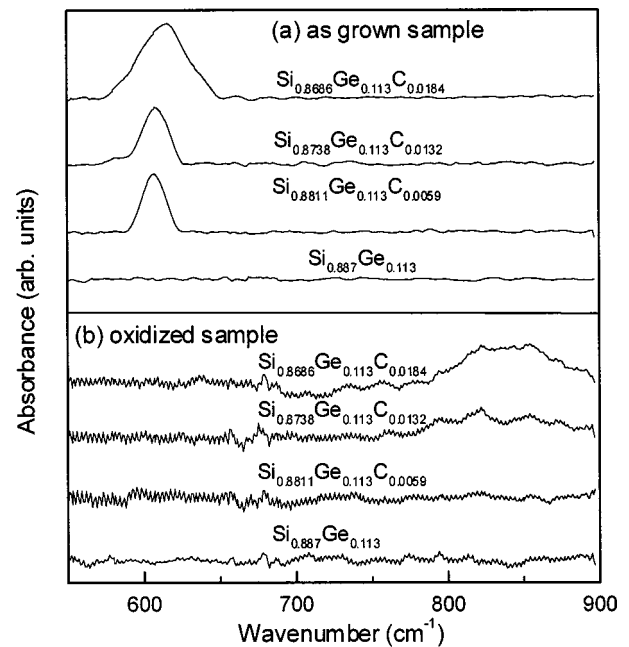


FIG. 1. Infrared absorption spectra of (a) as-prepared and (b) rapid thermal oxidized $\text{Si}_{0.887-y}\text{Ge}_{0.113}\text{C}_y$ and $\text{Si}_{0.8-y}\text{Ge}_{0.2}\text{C}_y$ layers formed by rapid thermal chemical vapor deposition technique.

$\text{Si}_{0.887}\text{Ge}_{0.113}$ shifts to $-\delta\theta$, indicating compressive perpendicular strain in the layer. The incorporation of C atoms into the $\text{Si}_{0.887}\text{Ge}_{0.113}$ layer decreases the average lattice constant and relaxes the strain. This is clearly shown by the shift of the diffraction peak towards the substrate Si peak in $\text{Si}_{0.8811}\text{Ge}_{0.113}\text{C}_{0.0059}$. Table I lists the strain of the samples calculated from the lattice constant obtained from the XRD

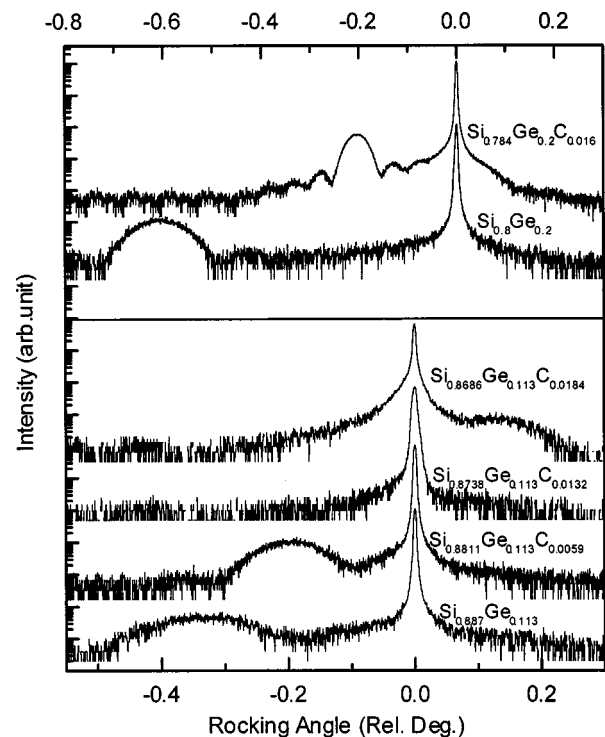


FIG. 2. (004) x-ray rocking curves of $\text{Si}_{0.887-y}\text{Ge}_{0.113}\text{C}_y$ and $\text{Si}_{0.8-y}\text{Ge}_{0.2}\text{C}_y$ layers formed by rapid thermal chemical vapor deposition technique.

TABLE I. The lattice mismatch strain of the as-prepared and rapid thermal oxidized $\text{Si}_{0.887-y}\text{Ge}_{0.113}\text{C}_y$ and $\text{Si}_{0.8-y}\text{Ge}_{0.2}\text{C}_y$ layers calculated from the x-ray diffraction results. The Ge and C concentrations of the as-prepared samples were estimated using the Vegard's rule.

Sample	Mismatch strain of films		Concentration	
	as-prepared (%)	oxidized (%)	Ge (%)	C (%)
$\text{Si}_{0.887}\text{Ge}_{0.113}$	0.46	0.41	11.14	0.00
$\text{Si}_{0.8811}\text{Ge}_{0.113}\text{C}_{0.0059}$	0.25	0.41	11.14	0.60
$\text{Si}_{0.8738}\text{Ge}_{0.113}\text{C}_{0.0132}$	0.017	0.41	11.14	1.30
$\text{Si}_{0.8686}\text{Ge}_{0.113}\text{C}_{0.0184}$	-0.23	0.51	11.14	2.04
$\text{Si}_{0.8}\text{Ge}_{0.2}$	0.83	0.82	19.92	0.00
$\text{Si}_{0.784}\text{Ge}_{0.2}\text{C}_{0.016}$	0.23	0.82	19.92	1.74

results. The Ge and C concentrations in Table I were also estimated from the XRD measurements using Vegard's law. Table I clearly shows that the strain of the as-prepared samples decrease with increase in the C concentration. Similar results are observed for samples $\text{Si}_{0.8}\text{Ge}_{0.2}$ and $\text{Si}_{0.784}\text{Ge}_{0.2}\text{C}_{0.016}$ in that a 1.6 at. % C has partially compensated the strain of the 20 at. % Ge film.

Note that in Fig. 2 there is only one single peak for $\text{Si}_{0.8738}\text{Ge}_{0.113}\text{C}_{0.0132}$ and this peak coincides with the substrate peak. This means that almost full strain compensation is obtained in this sample. Our calculation shows that the mismatch strain in this case is 0.017%. Osten *et al.*⁹ have calculated the amount of Ge to C for complete compensation in $\text{Si}_{1-x-y}\text{Ge}_x\text{C}_y$ system. According to their calculation, approximately 1.2 at. % C is required for full compensation of strain in a 11.3 at. % Ge sample. This is in good agreement with our XRD result of sample $\text{Si}_{0.8738}\text{Ge}_{0.113}\text{C}_{0.0132}$.

For $\text{Si}_{0.8686}\text{Ge}_{0.113}\text{C}_{0.0184}$, however, the peak appears at the right side of the substrate peak. This is due to the increase in C incorporation into the layer above complete compensation. This would result in tensile strain in the film.^{9,10} The mismatch strain is estimated to be -0.23%. Note that large amount of C incorporation leads to a crystallographic degradation of the layer. This may account for the shift and the broadening of the carbon peak in the IR spectrum of sample $\text{Si}_{0.8686}\text{Ge}_{0.113}\text{C}_{0.0184}$ in Fig. 1(a).

B. Rapid thermal oxidized samples

1. $\text{SiO}_2/\text{Si}_{1-x-y}\text{Ge}_x\text{C}_y$ interface

Figure 3(a) shows a montage of oxidized $\text{Si}_{0.8686}\text{Ge}_{0.113}\text{C}_{0.0184}$ sample. It can be seen from this figure that at the surface of the SiO_2 layer, there is a thin layer of GeO_2 (at binding energy 1221.43 eV). The existence of GeO_2 layer has been reported in the oxidation study of $\text{Si}_{1-x}\text{Ge}_x$ with $x > 50$ at. %, ¹⁶ or at low temperature, high pressure oxidation of $\text{Si}_{1-x}\text{Ge}_x$ films.¹⁷ Figure 3(b) is the XPS profile of the same sample as Fig. 3(a). It is not possible to see clearly the GeO_2 in Fig. 3(b) due to the thin layer and low concentration. No Ge can be found in the SiO_2 layer and there is a Ge pile-up at the $\text{SiO}_2/\text{Si}_{1-x-y}\text{Ge}_x\text{C}_y$ interface. These results are similar to those reported by Nayak *et al.*¹³ on rapid thermal oxidized $\text{Si}_{1-x}\text{Ge}_x$ strained layers. They reported a rejection of Ge in the oxide and a Ge-rich layer at the $\text{SiO}_2/\text{Si}_{1-x}\text{Ge}_x$ interface.

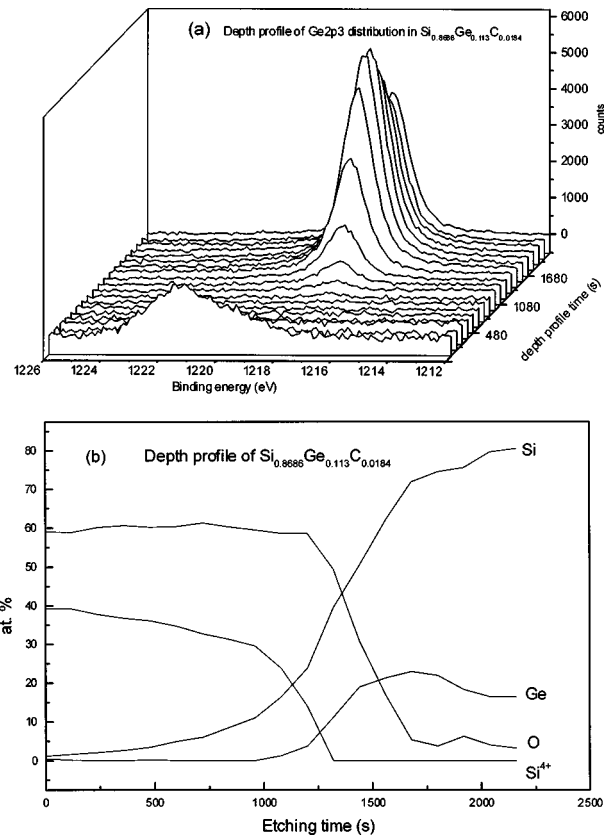


FIG. 3. (a) Montage of oxidized $\text{Si}_{0.8686}\text{Ge}_{0.113}\text{C}_{0.0184}$ samples, (b) XPS depth profiles of rapid thermal oxidized $\text{Si}_{0.8686}\text{Ge}_{0.113}\text{C}_{0.0184}$ sample. The carbon concentration is not shown here as it cannot be determined accurately from XPS measurements.

We have carried out electrical characterization¹⁸ of rapid thermal oxidized $\text{SiO}_2/\text{Si}_{1-x-y}\text{Ge}_x\text{C}_y$ interface and found that Ge segregation results in degradation of electrical properties of $\text{Al}/\text{SiO}_2/\text{Si}_{1-x-y}\text{Ge}_x\text{C}_y$ capacitors. The fixed oxide charge and interface trap densities were found to be in the range of $1.5 \times 10^{12} \text{ cm}^{-2}$ and $2 \times 10^{12} \text{ cm}^{-2} \text{ eV}^{-1}$, respectively. These values are very similar to that reported by Nayak *et al.*¹⁵ and LeGoues *et al.*¹⁹ on $\text{SiO}_2/\text{Si}_{1-x}\text{Ge}_x$ samples.

2. Structural characterization

The x-ray rocking curves of the rapid thermal oxidized samples are shown in Fig. 4. Note that the peak positions of $\text{Si}_{0.887}\text{Ge}_{0.113}$ and $\text{Si}_{0.8}\text{Ge}_{0.2}$ films remain unchanged after oxidation. This means that no relaxation of the perpendicular strain was observed in SiGe film. Note that Nayak *et al.*¹⁵ have also reported negligible strain relaxation in rapid thermal oxidized $\text{Si}_{0.8}\text{Ge}_{0.2}$ sample.

The XRD behavior of the oxidized $\text{Si}_{1-x-y}\text{Ge}_x\text{C}_y$ films depends on the amount of C in the as-prepared films. For films that were partially (i.e., show compressive strain) or fully compensated, the oxidation process reduces the C content in the film such that the oxidized films are similar to $\text{Si}_{1-x}\text{Ge}_x$ film. For instance, in Fig. 4, the peaks of oxidized $\text{Si}_{0.8811}\text{Ge}_{0.113}\text{C}_{0.0059}$ and $\text{Si}_{0.8738}\text{Ge}_{0.113}\text{C}_{0.0132}$ samples and $\text{Si}_{0.784}\text{Ge}_{0.2}\text{C}_{0.016}$ shifted close to the $\text{Si}_{0.887}\text{Ge}_{0.113}$ and $\text{Si}_{0.8}\text{Ge}_{0.2}$ peaks, respectively. Our calculation in Table I also

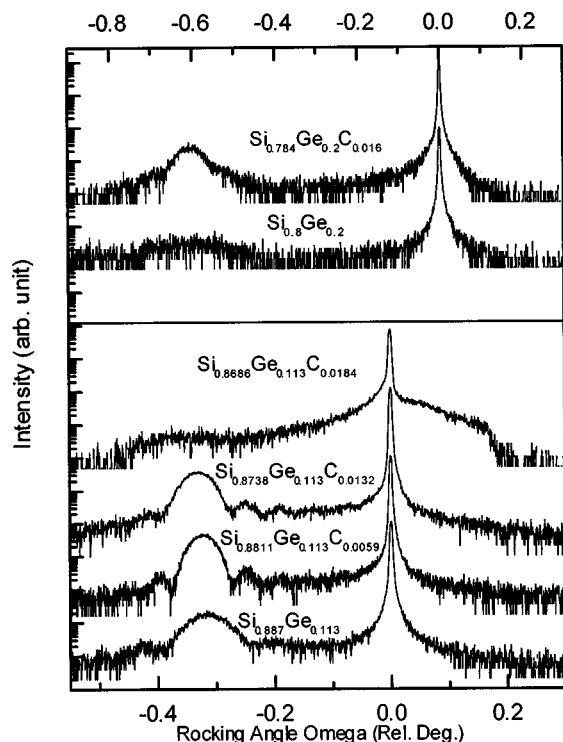


FIG. 4. (004) x-ray rocking curves of rapid thermal oxidized $\text{Si}_{0.887-y}\text{Ge}_{0.113}\text{C}_y$ and $\text{Si}_{0.8-y}\text{Ge}_{0.2}\text{C}_y$ samples. The rapid thermal oxidation process was carried out at 1000°C for 270 s in dry oxygen ambient.

shows that for oxidized $\text{Si}_{0.887-y}\text{Ge}_{0.113}\text{C}_y$ samples with $y \leq 0.0132$ and $\text{Si}_{0.784}\text{Ge}_{0.2}\text{C}_{0.016}$, the strain increases after oxidation and reaches a value same as that of the SiGe. This is reasonable as Bair *et al.*²⁰ shown that wet oxidation of amorphous SiGeC at 950°C for 5 h resulted in the oxidation of carbon and the out gas of carbon from the bulk. Note that out-diffusion of carbon by formation of CO or CO_2 from strained $\text{Si}_{1-y}\text{C}_y$ film during wet oxidation is also observed by Garrido *et al.*²¹ We will further discuss this point when we examine the SIMS results later.

For films with a higher C content which show tensile strain, the explanation of the XRD results of the oxidized sample is more complicated. For example, in Fig. 4, two distinct regions are observed on the left and right sides of the substrate peak for oxidized $\text{Si}_{0.8686}\text{Ge}_{0.113}\text{C}_{0.0184}$ sample. The two regions suggest the existence of compressive and tensile strain in the film. Comparing the “tensile” (i.e., right side) peaks of the as-prepared (see Fig. 2) and oxidized $\text{Si}_{0.8686}\text{Ge}_{0.113}\text{C}_{0.0184}$ samples, the peak seems to shift more towards the Si peak in the oxidized sample in that no clear peak can be observed in this sample. On the left side of the Si peak of oxidized sample, there appears to be a small peak at $\delta\theta \sim 0.4^\circ$ and a broadening region between $\delta\theta = -0.1$ and -0.3° . The broadening of x-ray rocking curve may be caused by an increase in defect density in the strained layer²² or interdiffusion.^{6,23} In Table I, a compressive strain of 0.51% was obtained for $\text{Si}_{0.8686}\text{Ge}_{0.113}\text{C}_{0.0184}$ and this is higher than that of the $\text{Si}_{0.887}\text{Ge}_{0.113}$.

Figure 1(b) shows the IR spectra of all the oxidized samples. Note that the substitutional carbon peak is absent in all the oxidized samples and a weak SiC stretching peak

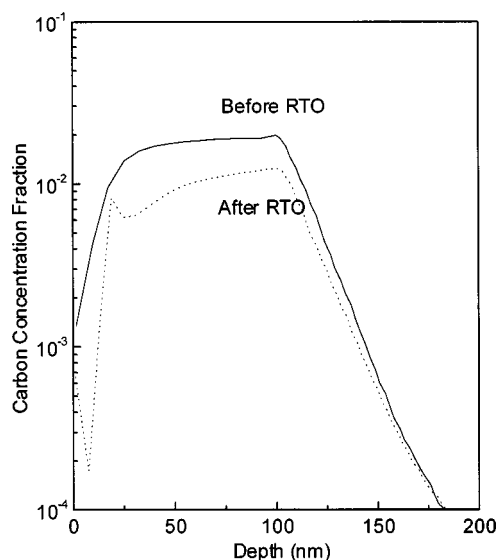


FIG. 5. SIMS profile of carbon in $\text{Si}_{0.8686}\text{Ge}_{0.113}\text{C}_{0.0184}$ sample before and after rapid thermal oxidation.

($\sim 850\text{ cm}^{-1}$) can be seen in $\text{Si}_{0.8686}\text{Ge}_{0.113}\text{C}_{0.0184}$. The higher strain value of the oxidized $\text{Si}_{0.8686}\text{Ge}_{0.113}\text{C}_{0.0184}$ sample may be due to the SiC precipitates in the film. The SiC precipitation can increase the vertical lattice constant due to the consumption of Si and C atoms during the formation of SiC precipitates. The increase of the vertical lattice constant by 1% of SiC formation in SiGeC is effectively the same as that by 8.3% of Ge incorporation.²⁴

A SIMS experiment was performed on oxidized $\text{Si}_{0.8686}\text{Ge}_{0.113}\text{C}_{0.0184}$ sample to examine the possible existence of the “two regions” suggested in the previous paragraph. Figure 5 shows the SIMS result (using Cs^+) of $\text{Si}_{0.8686}\text{Ge}_{0.113}\text{C}_{0.0184}$ sample before and after RTO. It can be seen from this figure that before RTO, the carbon concentration is uniform throughout the $\text{Si}_{0.8686}\text{Ge}_{0.113}\text{C}_{0.0184}$ layer. After RTO, the carbon concentration in the film has generally reduced. The peak indicates the segregation of carbon towards the oxide interface. It is also clear from Fig. 5 that the loss of substitutional carbon is enhanced near the $\text{SiO}_2/\text{SiGeC}$ interface. For depth 50–100 nm, the carbon concentration is constant at ~ 1.24 at.%. This layer may account for the tensile strain in the RTO film as shown in Fig. 4. The carbon concentration at the first 50 nm is characterized by a peak followed by a graded region. This rather complicated distribution may be responsible for the compressive strain in Fig. 4 of RTO $\text{Si}_{0.8686}\text{Ge}_{0.113}\text{C}_{0.0184}$ sample. The results in Fig. 5 show clearly that high-temperature oxidation reduces the carbon content in the $\text{Si}_{1-x-y}\text{Ge}_x\text{C}_y$ system, in good agreement with the suggestions of Bair *et al.*²⁰ and Garrido *et al.*²¹

Note that conventional annealing of partially strain compensated $\text{Si}_{1-x-y}\text{Ge}_x\text{C}_y$ films at high temperature ($>800^\circ\text{C}$) resulted in a total loss of substitutional C due to the formation of SiC.^{24–28} Warren *et al.*²⁸ reported various degree of SiC formation during high-temperature rapid thermal annealing of SiGeC films in N_2 ambient. This is, however, vary different from our case in that our ambient was

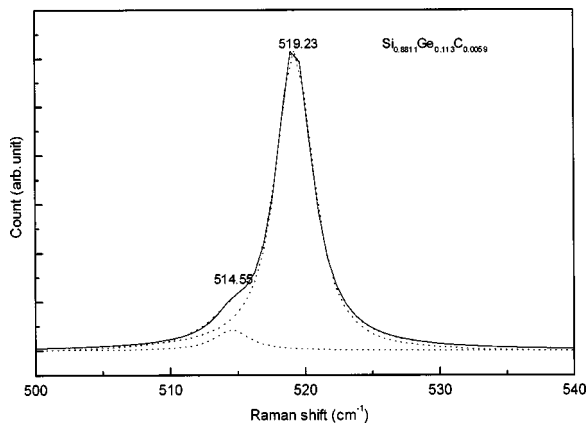


FIG. 6. Typical room temperature Raman spectrum of $\text{Si}_{0.8811}\text{Ge}_{0.113}\text{C}_{0.0059}$ sample. The dashed lines are the individual components that correspond to the Si–Si vibrations of the substrate and that of the alloy layer.

dry oxygen. The carbon atoms in the SiGeC film would react with oxygen to form CO or CO_2 , thus reduce the chances of forming SiC. This may account for the fact that we can only observed weak SiC peak in the IR spectrum of oxidized $\text{Si}_{0.8686}\text{Ge}_{0.113}\text{C}_{0.0184}$ sample.

The Raman spectra of our samples show a strong Si substrate peak at 520 cm^{-1} . The weaker peaks at 430, 408, and 300 cm^{-1} are the two Si–Ge and the Ge–Ge modes of the alloy. The peak at 610 cm^{-1} is due to substitutional C in Si. Figure 6 shows a typical Si–Si Raman spectrum of the $\text{Si}_{0.8811}\text{Ge}_{0.113}\text{C}_{0.0059}$ samples. Note that the Si–Si line can be deconvoluted into two components, i.e., from the Si substrate and from the $\text{Si}_{0.8811}\text{Ge}_{0.113}\text{C}_{0.0059}$ layer. The peak at lower energy side corresponds to the Si–Si mode from the alloy layer.

Figure 7 shows the separation between the Si–Si peaks of the alloy and Si substrate as a function of the C concentration in $\text{Si}_{1-x-y}\text{Ge}_x\text{C}_y$ films before and after oxidation. It can be seen for both the 11.3 and 20 at. % Ge samples, the distance between the two Si–Si peaks of the as-prepared samples increases with increase in C concentration. This is expected as the addition of C in the $\text{Si}_{1-x}\text{Ge}_x$ layer leads to

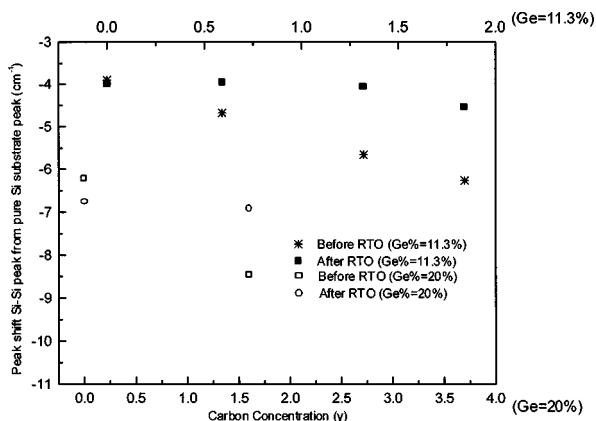


FIG. 7. Peak positions of the Si–Si Raman line of as-prepared and oxidized $\text{Si}_{0.887-y}\text{Ge}_{0.113}\text{C}_y$ and $\text{Si}_{0.8-y}\text{Ge}_{0.2}\text{C}_y$ samples relative to the Raman line of pure Si as a function of carbon concentration (y).

a partial relaxation of the Si–Si bonds towards their geometrical arrangement in the bulk Si.²⁹

It is interesting to note that RTO process reduces the separation between the two peaks of samples $\text{Si}_{0.8811}\text{Ge}_{0.113}\text{C}_{0.0059}$ and $\text{Si}_{0.8738}\text{Ge}_{0.113}\text{C}_{0.0132}$ to that close to $\text{Si}_{0.887}\text{Ge}_{0.113}$. Note these are partially (compressive) or fully compensated samples, the Raman results are in good agreement to our discussion of XRD results of Fig. 4. For $\text{Si}_{0.8686}\text{Ge}_{0.113}\text{C}_{0.0184}$ (tensile) sample, the reduction is only partial and this is basically due to the higher carbon concentration in this sample.

IV. CONCLUSIONS

In summary, the structural properties of as-prepared and rapid thermal oxidized RTCVD grown $\text{Si}_{1-x-y}\text{Ge}_x\text{C}_y$ alloy films have been investigated using the XRD, XPS, SIMS, and Raman spectroscopy techniques. Incorporating C into the $\text{Si}_{1-x-y}\text{Ge}_x\text{C}_y$ system can either partially, fully or over compensates the strain in the layers.

The structural properties of the oxidized $\text{Si}_{1-x-y}\text{Ge}_x\text{C}_y$ films depends on the C content of the as-prepared films. For films with C content equal or below fully compensation, RTO reduces the C content such that the oxidized films resemble close to that of the $\text{Si}_{1-x}\text{Ge}_x$ film. For film with C content that gives tensile strain, RTO will reduce the C content such that two broad regions exist in the film. The region with C content higher than that required for full strain compensation (albeit less than original concentration) accounts for the broad tensile peaks in the XRD results. The other region with lower C content is responsible for the broad compressive peaks. The results from Raman spectroscopy on the Si–Si strain confirm qualitatively our XRD observation.

ACKNOWLEDGMENTS

The authors wish to thank the National University of Singapore for the provision of a research fellowship (J.H.C. and L.K.B.) and scholarship (F.W.). They would also like to express their gratitude to the National Science and Technology Board for a research grant for this work (No. GR6471).

- ¹S. C. Jain, in *Advances in Electronics and Electron Physics*, Supplement 24, edited by P. W. Hawkes (Academic, San Diego, CA, 1994).
- ²G. L. Patton *et al.*, *IEEE Electron Device Lett.* **11**, 171 (1990).
- ³R. Karunasiri, J. S. Park, and K. L. Wang, *Appl. Phys. Lett.* **59**, 2588 (1991).
- ⁴Y. Rajakarunayake and T. McGill, *J. Vac. Sci. Technol. B* **8**, 929 (1990).
- ⁵Y. Mii, Y. Xie, E. Fitzgerald, D. Monroe, F. Thiel, B. Weir, and L. Feldman, *Appl. Phys. Lett.* **59**, 1611 (1991).
- ⁶A. T. Fiory, J. C. Bean, R. Hull, and S. Nakahara, *Phys. Rev. B* **31**, 4063 (1985).
- ⁷C. A. King, L. J. Hoyt, D. B. Noble, C. M. Gronet, J. F. Gibbons, M. P. Scott, T. I. Kamins, and S. S. Laderman, *IEEE Electron Device Lett.* **10**, 150 (1989).
- ⁸E. Eberl, S. S. Iyer, S. Zollner, J. C. Tsang, and F. K. LeGoues, *Appl. Phys. Lett.* **60**, 3033 (1992).
- ⁹H. J. Osten, E. Bugiel, and P. Zaumseil, *Appl. Phys. Lett.* **64**, 3440 (1994).
- ¹⁰J. Mi, P. Warren, P. Letourneau, M. Judelewicz, M. Gailhanou, M. Dutoit, C. Dubois, and J. C. Dupuy, *Appl. Phys. Lett.* **67**, 259 (1995).
- ¹¹R. Singh, *J. Appl. Phys.* **63**, R59 (1988).
- ¹²J. C. Bean, A. T. Fiory, R. Hull, and R. T. Lynch, in *Proceedings of the 1st International Symposium on Silicon Molecular Beam Epitaxy*, edited by J. C. Bean (Electrochemical Society, Pennington, NJ, 1985).

- ¹³D. K. Nayak, K. Kamjoo, J. C. S. Woo, J. S. Park, and K. L. Wang, *Appl. Phys. Lett.* **56**, 66 (1990).
- ¹⁴D. K. Nayak, K. Kamjoo, J. S. Park, J. C. S. Woo, and K. L. Wang, *Appl. Phys. Lett.* **57**, 369 (1990).
- ¹⁵D. K. Nayak, K. Kamjoo, J. S. Park, J. C. S. Woo, and K. L. Wang, *IEEE Trans. Electron Devices* **39**, 56 (1992).
- ¹⁶J. Eugege, F. K. LeGoues, V. P. Kesan, S. S. Iyer, and F. M. d'Heurle, *Appl. Phys. Lett.* **59**, 78 (1991).
- ¹⁷D. C. Paine, C. Caragianis, and A. F. Schwartzman, *J. Appl. Phys.* **70**, 5076 (1991).
- ¹⁸J. Mi, H. Yoong, F. Zhang, C. Y. Yang, J. H. Chen, and W. K. Choi, *ESSDERC'99* (submitted).
- ¹⁹F. K. LeGoues, R. Rosenberg, T. Nguyen, F. Himpsel, and B. S. Meyer-son, *J. Appl. Phys.* **65**, 1724 (1989).
- ²⁰A. E. Bair, Z. Atmon, T. L. Alford, and D. J. Smith, *J. Appl. Phys.* **83**, 2835 (1998).
- ²¹B. Garrido, J. Morante, M. Franz, K. Pressel, D. Krüger, P. Zaumseil, and H. J. Osten, *J. Appl. Phys.* **85**, 833 (1999).
- ²²T. Vreeland and B. M. Paine, *J. Vac. Sci. Technol. A* **4**, 3153 (1986).
- ²³D. C. Houghton, D. D. Perovic, J.-M. Baribeau, and G. C. Weatherly, *J. Appl. Phys.* **67**, 1850 (1990).
- ²⁴C. W. Liu, Y. D. Tseng, M. Y. Chern, C. L. Chang, and J. C. Sturm, *J. Appl. Phys.* **85**, 2124 (1999).
- ²⁵J. W. Strane, S. T. Picraux, H. J. Stein, S. R. Lee, J. Candelaria, D. Theodore, and J. W. Mayer, *Mater. Res. Soc. Symp. Proc.* **321**, 467 (1994).
- ²⁶G. G. Fischer, P. Zaumseil, E. Bugiel, and H. J. Osten, *J. Appl. Phys.* **77**, 1934 (1995).
- ²⁷K. Pressel, G. G. Fischer, P. Zaumseil, M. Kim, and H. J. Osten, *Thin Solid Films* **294**, 133 (1997).
- ²⁸P. Warren, J. Mi, F. Overney, and M. Dutoit, *J. Cryst. Growth* **157**, 414 (1995).
- ²⁹J. Menéndez, P. Gopalan, G. S. Spencer, N. Cave, and J. W. Strane, *Appl. Phys. Lett.* **66**, 1160 (1995).